

AD-A058 446

CALIFORNIA INST OF TECH PASADENA

DETERMINATION OF MICROSCOPIC ATOMIC STRUCTURE OF SURFACES AND O--ETC(U)

AUG 78 W H WEINBERG

DAHCO4-75-G-0170

F/G 20/12

NL

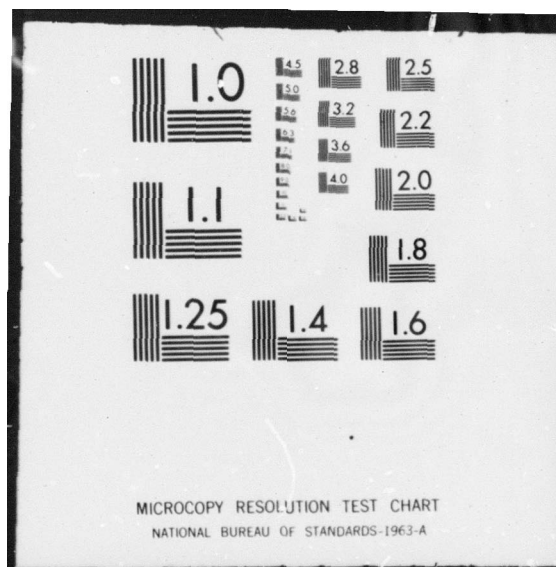
UNCLASSIFIED

ARO-13120.1-C

| OF |
AD
A058446



END
DATE
FILMED
11-78
DDC



UDC FILE COPY: ADA 058446

UNCLASSIFIED		SECURITY CLASSIFICATION OF THIS PAGE (When Data Entered)	
REPORT DOCUMENTATION PAGE			
1. REPORT NUMBER	2. GOVT ACCESSION NO.	3. RECIPIENT'S CATALOG NUMBER	
13120.1-C	18 ARO		
4. TITLE (and Subtitle)		5. TYPE OF REPORT & PERIOD COVERED	
Determination of Microscopic Atomic Structure of Surfaces and Overlayers which are Important in Heterogeneous Catalysis.		Final Report 15 Jun 75 - 14 Jun 78	
6. AUTHOR(s)		7. PERFORMING ORG. REPORT NUMBER	
W. Henry Weinberg			
8. CONTRACT OR GRANT NUMBER(s)		9. PROGRAM ELEMENT, PROJECT, TASK AREA & WORK UNIT NUMBERS	
		DAHC04-75-G-0170 DAAG-29-75-0-0170	
10. PERFORMING ORGANIZATION NAME AND ADDRESS		11. REPORT DATE	
California Institute of Technology Pasadena, California 91125		Aug 78	
12. CONTROLLING OFFICE NAME AND ADDRESS		13. NUMBER OF PAGES	
U. S. Army Research Office P. O. Box 12211 Research Triangle Park, NC 27709		22	
14. MONITORING AGENCY NAME & ADDRESS (if different from Controlling Office)		15. SECURITY CLASS. (of this report)	
		unclassified	
		15a. DECLASSIFICATION/DOWNGRADING SCHEDULE	
16. DISTRIBUTION STATEMENT (of this Report)			
Approved for public release; distribution unlimited.			
12 23 p.			
17. DISTRIBUTION STATEMENT (of the abstract entered in Block 20, if different from Report)			
18. SUPPLEMENTARY NOTES			
The findings in this report are not to be construed as an official Department of the Army position, unless so designated by other authorized documents.			
19. KEY WORDS (Continue on reverse side if necessary and identify by block number)			
20. ABSTRACT (Continue on reverse side if necessary and identify by block number) This report describes the research efforts in five different areas, all related to a better understanding of solid surfaces: (1) The analysis of surface structures by low-energy electron diffraction (LEED); (2) Other research related to LEED such as an improved method of measuring experimentally the angle of incidence of the electron beam in a LEED apparatus; (3) An examination of desorption phenomena including a theoretical treatment of thermal desorption mass spectrometry (TDS); (4) Model calculations concerning the dependence of the spectral intensity upon adsorbate concentration in inelastic electron tunneling spectroscopy (IETS); and (5) Chemisorption and surface reactions.			

LEVEL II

DDC
FORM 1
SEP 7 1978
F

Final Technical Report of
Research Agreement No. DAAG29-75-G-0170

DBC	B.H. Section	<input checked="" type="checkbox"/>
UNANNOUNCED		<input type="checkbox"/>
JUSTIFICATION		
BY	DISTRIBUTION/AVAILABILITY CODES	
D.		
A		

A. Introduction

This report serves to describe the research accomplished under the support of ARO Grant DAHC04-75-G-0170. Our efforts have focused in five different areas, all related to a better understanding of solid surfaces:

(1) The analysis of surface structures by low-energy electron diffraction (LEED) using both full multiple scattering (dynamic) and transform-convolution (kinematic) numerical schemes; (2) Other research related to LEED such as an improved method of measuring experimentally the angle of incidence of the electron beam in a LEED apparatus, the measurement of surface and bulk Debye temperatures, and the evaluation of adparticle-adparticle interaction energies via a measurement of order-disorder phenomena using LEED; (3) An examination of desorption phenomena including a theoretical treatment of thermal desorption mass spectrometry (TDS) and experimental measurements of electron stimulated desorption (ESD); (4) Model calculations concerning the dependence of the spectral intensity upon adsorbate concentration in inelastic electron tunneling spectroscopy (IETS), the change in electronic free energy upon reconstruction of an ideal (1x1) surface structure to either a reconstructed (2x1) or c(2x2) structure, and the change in the electronic density of states when a two-level adsorbate interacts with the s-band of the (100) surface of an fcc metal; and (5) Chemisorption and surface reactions, in particular, H₂, O₂ and CO on the (111) surface of Rh, and CO on the (110) surface of Ir. Each of these topics will be summarized in more detail in sections B through

78 09 01 007

F below. References cited in these sections are to the publications which have resulted from this grant support. For convenience, these references are listed separately in section G.

B. Analysis of Surface Structures by LEED

The *major* thrust of the research supported by this grant during the past three years has been concerned with a determination of the structure of solid surfaces. This includes both the relaxation (if present) of clean metallic surfaces as well as the position of ordered adatoms on metallic surfaces. This research has been both of a theoretical and an experimental nature. On the theoretical side, there have been two major advances, namely, the development of a transform-convolution method of analysis of the structure of clean surfaces via the direct analysis of LEED intensity-voltage (I-V) beam profiles, and the ability to perform full multiple scattering (dynamic) calculations for both clean surfaces and surfaces on which there are ordered overlayers. The latter ability is due entirely to Dr. Michel Van Hove who spent one year in our research group at Caltech as a postdoctoral fellow prior to moving to the University of Munich. On the experimental side, LEED I-V beam profiles have been measured for clean surfaces and surfaces with ordered overlayers, in particular, the Ir(111), Ir(110), Rh(111) and Ni(111) surfaces.

The formulation of a direct method of analyzing LEED I-V beam profiles

to arrive at surface relaxation via a Fourier transform method involved the following features: (1) The inner potential, V_0 , which is crucial for converting energy to momentum transfer, is treated as a variable to be determined rather than as a known input parameter. (2) Rather than deconvolute the Patterson function (which leads to instabilities), a calculated convolution product is compared with the observed Patterson function. (3) The convolution product is the convolution of a "window" function and a series of delta functions representing the layer positions. The layer positions are chosen arbitrarily, and then the amplitudes of the delta functions are obtained by performing a least squares fit of the convolution product to the observed Patterson function. (4) The mean square deviation of this fitted convolution product with the observed Patterson function is calculated. (5) Finally, this deviation (called the residual) is plotted as a function of both V_0 and the degree of relaxation (t) of the surface layer. The value of t for which the minimum occurs in the residual gives the surface structure in the I-V profiles in the sense that as the multiple scattering structure increases, the ability to determine the structure diminishes gradually, not suddenly.

This method has been illustrated fully using "model" kinematic I-V data from a surface which is both relaxed and unrelaxed (1). It was found that even ideal "data" cannot be analyzed to give an "exact" solution, i.e., a perfect fit between the Patterson function of the kinematic data and the convolution product of the window transform function and the series of delta functions representing the crystal layer spacing. Nevertheless, it was shown that the method is capable of determining relaxations even from data which are highly dynamic. This was illustrated by analyzing the theoretical I-V profiles of the (00), (11), (02) and (20) beams from the clean W(110)

surface calculated by M. A. Van Hove and S. Y. Tong using a multiple scattering program (1, 2, 3). The correct structure was determined for surface relaxations of + 9%, 0% and - 9%. These results were important in that they showed how the data range in LEED affects one's ability to determine surface relaxation, that the uncertainties in the theory are not sufficient to destroy the ability to determine the structure, and that the method is capable of resolving relaxations on the order of $\pm 5\%$ which is comparable to the uncertainty in multiple scattering analyses.

Next, the transform-convolution method was applied to experimental data from the (111) surface of Ir measured in our laboratory. Multiple scattering calculations were performed also to determine the relaxation of this surface for the first time (4, 5). Seven specular I-V beam profiles were measured from 15 to 975 eV at incident angles from 7° to 62.5° relative to the surface normal. The transform-convolution method of analysis showed that the outermost layer of Ir(111) is either unrelaxed or contracts by at most 4% of the bulk spacing. In agreement with this, the dynamic calculations indicated a contraction of $2.5 \pm 5\%$. The dynamic calculations showed also that the registry of the first layer of this crystal surface is not shifted, maintaining the fcc structure.

Published experimental data for the (110) surface of the fcc metals Ni, Al and Ag were analyzed using the transform-convolution method since earlier dynamic calculations had indicated a contraction of each of these surfaces. The results of the transform-convolution analysis indicated that the first layer spacing of Ni(110), Al(110) and Ag(110) is contracted by 5%, 4% and 7% of the bulk spacing, respectively (4, 6). These results are in good agreement with the results which had been obtained previously using dynamic calculations.

In a similar study, both specular and nonspecular LEED I-V beam profiles were measured for the Rh(111) surface in our laboratory, and the surface relaxation was determined using both the transform-convolution method and dynamic calculations (7). Within experimental error, neither expansion nor contraction of the topmost layer was detected. The results of the transform-convolution analysis of specular beams at two angles of incidence and of a nonspecular beam at normal incidence suggested an expansion of the topmost layer of $3 \pm 5\%$ of the bulk layer spacing. In agreement with this, comparisons between the results of the dynamical calculation and the experimental data for five nonspecular beams at normal incidence suggested that the surface layer relaxes by $0 \pm 5\%$. In addition, the dynamic calculations indicated that the topmost layer maintains an fcc structure.

Two other clean surface structures have been analyzed using multiple scattering calculations, the Co(001) surface^{*} and the unreconstructed Ir(110) surface. The surface structure of Co(001) was examined in order to determine the existence of residual surface phases or "frozen in" surface embryos responsible for the nucleation of the Martensitic transformation in Co (8). It was found that no such residual surface embryos exist, and that the structural phase of the surface is equivalent to the respective allotropic phase of the bulk. Moreover, the transformation at the surface was observed to be strongly first-order with significant temperature hysteresis.

An Ir(110) - (1x1) surface structure was prepared by adsorbing a quarter-monolayer of oxygen at 575 K on a clean, reconstructed (1x2) surface (9). A

*The experiments were performed by A. Ignatiev *et al.* at the University of Houston, and the calculations were performed by M. A. Van Hove at Caltech.

comparison between measured and dynamically calculated LEED I-V beam profiles indicated that the oxygen is distributed randomly over the crystal surface, and the (1x1) structure is the same as a clean unreconstructed (1x1) structure with a topmost interlayer Ir spacing of $1.26 \pm 0.05 \text{ \AA}$. This is equivalent to a contraction of approximately 7.5% of the bulk interlayer spacing of 1.36 \AA .

Dynamic calculations were performed successfully in order to determine the locations of hydrogen atoms on a Ni(111) surface marking the first determination of the structure of a hydrogen overlayer on any surface (10, 11, 12). Hydrogen adsorption below room temperature on Ni(111) yielded the appearance of a (2x2) overlayer structure of which the "extra" beams attained a maximum intensity after an exposure of approximately 2.5×10^{-6} torr-sec. A further increase in the exposure led to a gradual weakening and finally complete disappearance of the superstructure. I-V beam profiles were measured at maximum intensity at a surface temperature of 110 K with normal incidence of the primary beam. These beam profiles were analyzed by dynamic calculations using reverse scattering perturbation theory in conjunction with renormalized forward scattering and layer doubling. The Ni substrate was found to be unaffected by the presence of the hydrogen atoms which are arranged in a graphitic-like overlayer structure with a (2x2) unit cell, i.e., both types of threefold hollow sites on this fcc(111) surface are occupied. No detectable buckling of the hydrogen overlayer was observed to occur. The overlayer-substrate spacing was found to be $1.15 \pm 0.1 \text{ \AA}$, implying a Ni-H bond length of $1.84 \pm 0.06 \text{ \AA}$.

Finally, dynamic calculations have been carried out to determine the location of the oxygen atoms in a c(2x2) overlayer structure on the unreconstructed (110) surface of Ir (13). The ordered c(2x2) oxygen structure

was prepared by chemisorbing a half-monolayer of oxygen at room temperature on an unreconstructed (1x1) Ir(110) surface stabilized by a quarter-monolayer of randomly adsorbed oxygen. Results of the structural analysis showed that the ordered oxygen atoms are residing on the short-bridged sites (along the rows) on the (110) surface. The ordered overlayer-substrate interlayer spacing was found to be $1.37 \pm 0.05 \text{ \AA}$, corresponding to an Ir-O bond length of $1.93 \pm 0.07 \text{ \AA}$. The topmost substrate interlayer spacing was found to be $1.33 \pm 0.07 \text{ \AA}$, rather than $1.26 \pm 0.07 \text{ \AA}$ which is the topmost interlayer spacing of the unreconstructed (1x1) Ir(110) surface.

C. Other LEED Results

In other LEED work, not related to determining surface structures, three contributions have been made. First, a photographic technique has been developed which allows an easy and accurate determination of both the polar and azimuthal angles of incidence in a LEED experiment (14). This method involves analyzing the positions of the diffraction spots on a photograph of the LEED pattern. The position of a single spot defines uniquely the polar angle (with respect to the surface normal) and the azimuthal angle (with respect to an arbitrarily defined axis in the plane of the crystal surface). A computer program has been developed which uses as input data the beam energy, the beam label [the value of (hk)], the spot position on the photograph, the geometry of the apparatus, and the location of the camera. The program corrects for distortions caused by the camera and gives both angles determined by each spot as well as the uncertainties due to the inability to determine the spot position exactly. For a single setting of the crystal manipulator, several photographs can be obtained at different values of the

incident energy; and from a single photograph, typically on the order of ten spots can be analyzed. Using this large number of angle determinations, absolute accuracies better than 0.1° for both polar and azimuthal incidence angles are obtained routinely.

Second, the Debye temperature of the Rh(111) surface as well as that of bulk Rh has been measured by LEED (7). The determination of the Debye temperature (or, equivalently, the mean square displacement of the atoms due to thermal vibrations) is made by measuring the slope of the logarithm of the intensity of the specularly diffracted beam as a function of temperature. In the Debye temperature measurement of Rh(111), specular LEED beam intensities at several incidence angles were monitored as a function of temperature over a range of electron energies from approximately 30 eV to 1000 eV. It was found that the bulk Debye temperature is 380 ± 23 K (determined in the limit of high incident beam energy), and the normal component of the Debye temperature at the lowest electron energy used is 197 ± 12 K. The latter may be associated with the normal component of the surface Debye temperature.

Third, a Monte Carlo simulation has been carried out to describe two-dimensional order-disorder phenomena measured by LEED (15, 16). The model contains (attractive) first, (repulsive) second, and (attractive) third neighbor pairwise interactions. The special case of oxygen chemisorption on a W(110) surface (using the experimental data of T.-M. Lu, G.-C. Wang and M. G. Lagally), on which an ordered $p(2 \times 1)$ overlayer is formed at low surface temperatures, was considered explicitly. From the measured order-disorder transition temperatures at both quarter- and half-monolayer surface coverages, (non-unique) values of the three pairwise interaction energies were determined. These pairwise interaction energies were used to determine the variation in

the total interaction energy, the heat capacity and the entropy with surface temperature.

D. Desorption Phenomena

Desorption from solid surfaces has been investigated from two different points of view, both thermal desorption and electron beam stimulated desorption. First, a theoretical analysis of thermal desorption mass spectrometry (TDS) was performed from the point of view of appropriate dimensionless quantities (17). Analytical expressions were derived which allow a determination of the activation energy of desorption and the pre-exponential factor of the desorption rate coefficient using parameters obtained easily from thermal desorption mass spectra. In particular, it was demonstrated that the spectral peak widths and the temperature at which the maximum rate of desorption occurs may be used to describe both first and second order desorption kinetics. The use of the method was illustrated explicitly by applying it to the analysis of several important classes of desorption reactions. Then, the distortions which are associated with TDS as a result of the combined effect of surface heating rate and system pumping speed were quantified theoretically (18). It was demonstrated that considerable error in the determination of the activation energy and the pre-exponential factor of desorption can be introduced by the combined effects of high heating rate and low pumping speed. It was found that for an accurate determination of the activation energy and the pre-exponential factor for first-order desorption, the reciprocal of the product of the heating rate and the pumping time constant must be rather large, e.g., greater than approximately 0.5.

The other aspect of desorption which was considered is the case of ESD.

Since the electron beam used as a probe in electron scattering experiments such as LEED and Auger electron spectroscopy (AES) may perturb a chemisorbed overlayer, it is imperative to investigate this effect. For this reason, electron beam induced perturbations of CO chemisorbed on Ir(111) were measured experimentally using LEED and AES (19). The total interaction cross section for electron stimulated desorption and dissociation was found to be approximately 0.8 to $1.7 \times 10^{-17} \text{ cm}^2$ when defined with respect to the primary flux of a 2.5 keV electron beam. Electron stimulated dissociation was found to occur at 1-2% of the rate of electron stimulated desorption.

E. Model Calculations: Inelastic Electron Tunneling Spectroscopy, Surface Reconstruction, Changes in Electronic Densities of States

A theory was developed which describes the dependence of the spectral intensity upon adsorbate concentration in inelastic electron tunneling spectroscopy (20 - 22). In contrast to previous theories which predicted a linear dependence, it was shown that the intensity of molecular vibrational loss peaks varies approximately as $n^{1.3}$, where n is the concentration of adsorbate on the insulator surface in a metal-insulator-metal tunneling junction. The actual dependence does not follow a simple power law, but over the range of from 5% to 90% of saturation coverage, the dependence can be approximated by $n^{1.3}$. This result is in agreement with experimental measurements of J. Langan and P. Hansma who examined benzoic acid chemisorption on an aluminum oxide surface. This model makes it possible to use intensity measurements to determine relative coverages on the surface, and, consequently, evaluate the kinetics of adsorption.

A Green's function perturbation technique was developed which is appropriate for obtaining the change in the total electronic energy when the surface atoms of a crystal reconstruct in a periodic manner (23). The phase shift technique was used to determine the change in the electronic density of states. The method is quite general and can be used to study arbitrary surfaces which are reconstructed. As a specific example, the change in the total electronic energy which occurs upon reconstruction of the (001) surface of a model two-band crystal with the CsCl structure was calculated (24). The energy changes due to a (2x1) and a c(2x2) reconstruction were considered. The occurrence of reconstruction on a surface was shown to be dependent upon the relative magnitudes of the electronic energy and the elastic strain energy.

Finally, a model calculation was carried out for the orbital density of states, as well as the change in the density of states due to the chemisorption, of a two-level adsorbate bonded to the s-band of an fcc(100) metal surface (25). The calculation was carried out for an adsorption geometry with the adatom situated over the four-fold hole site, with a π -bonding interaction with the diagonal substrate atoms. A Green's function formalism was used within the LCAO-tight binding approximation. It was found that orbital resonances contain not only contributions from the adorbitals but also from the substrate group orbital which participates in the bonding. The admixture of each orbital in the resonances can be understood qualitatively in terms of both direct and indirect interactions which depend on the parameters of the model, namely, the unperturbed adorbital energies, the adsorbate-substrate coupling strengths, and the intra-adsorbate coupling strength.

F. Chemisorption and Surface Reactions

In addition to surface structural determinations, recent efforts have focused strongly on investigations of chemisorption and surface reaction kinetics. This work will continue with the support of a renewal proposal now under review by the ARO. Work already completed in this area includes the refinement of a method of measuring work function changes continuously and a study of the chemisorption of CO on the (110) surface of Ir.

First, a method was developed for measuring work function changes continuously (26). It is an ac variation of the diode technique and can be implemented easily in a standard retarding potential LEED/Auger system with derivative detection. Measurements for oxygen adsorption on the (110) surface of Ir were made to illustrate that this method can resolve work function changes within 5 meV.

Also, the chemisorption of CO on well-characterized clean and oxidized Ir(110) surfaces was studied in an ultrahigh vacuum environment (27). On both surfaces, it was found that adsorption occurs via a mobile precursor state. At surface temperatures of both 90 and 300 K, the adsorption kinetics were shown to be independent of whether the surface is clean or oxidized. Both LEED and thermal desorption data indicated that saturation coverage is approximately 10^{15} molecules/cm², or one monolayer under all conditions. No evidence for physical adsorption of CO was found, even at 90 K, at which temperature the probability of adsorption is nearly unity until saturation coverage is reached. At 300 K, the probability of adsorption was found to be unity at low surface coverages but decreased dramatically at 0.8 of saturation coverage. This decrease was attributed to interadsorbate repulsion. A kinetic model was formulated which suggests that a repulsive interaction of 2 kcal/mole exists between CO molecules at that fractional surface coverage.

To this point, that work which has been completed has been summarized. In addition, a significant amount of experimental information has been measured for the adsorption of H_2 , CO and O_2 ; the nonreactive coadsorption of H_2 and O_2 , and H_2 and CO; and the reactive coadsorption of H_2 and O_2 on the (111) surface of Rh. Results to date will be presented below, although this work will be completed, and manuscripts will be prepared with the support of the renewal grant.

1. The Adsorption of Oxygen on the (111) Surface of Rhodium, P. A. Thiel, J. T. Yates, Jr. and W. H. Weinberg (in preparation).

The adsorption of oxygen on Rh(111) at 100 K has been studied by TDS, AES and LEED. Oxygen adsorbs into a disordered state at 100 K and orders irreversibly into an apparent (2x2) surface structure upon heating to temperatures above 150 K. On the (111) surface, this could either be a true (2x2) overlayer or three independent domains of (2x1) structures rotated 120° with respect to one another. LEED I-V data have been collected, and a dynamic LEED calculation will be performed to clarify the structure of the "(2x2)" oxygen overlayer. The kinetics of ordering of the oxygen have been measured at surface temperatures between 150 and 280 K by monitoring the intensity of the $(1, \frac{1}{2})$ LEED beam as a function of time at various surface temperatures. The kinetic data are consistent only with a model in which the rate of ordering of oxygen adatoms is proportional to the square of the concentration of disordered oxygen. The activation energy for ordering was found to be 13.5 ± 0.5 kcal/mole. The fact that the ordering kinetics are proportional to the square of the concentration of disordered oxygen may

well be due to the nature of the interactions among the oxygen adatoms on the surface, e.g., the addition of a single adatom to the ordered structure may be energetically unfavorable compared to the concerted addition of two adatoms to the ordered structure. This point of view will be formulated quantitatively in an effort to explain the unexpected second order kinetics which were observed. At surface temperatures above 280 K, the oxygen undergoes a two-step irreversible disordering and dissolution process. Formation of the high temperature disordered state is retarded at high coverages of oxygen on the surface.

The TDS and AES data show also that oxygen adlayers are depleted by dissolution into the bulk of the Rh at temperatures above 400 K. The thermal desorption of oxygen shows a "threshold effect", with no desorption of oxygen occurring below an exposure of approximately 1.3×10^{-6} torr-sec, even though a significant quantity of oxygen chemisorbs at lower exposures as judged by AES. Analysis of the thermal desorption data at rather low surface coverages (extrapolated to zero coverage) yields values of the pre-exponential factor of the (second order) desorption rate coefficient and the activation energy of desorption of 2.5×10^{-3} cm²/sec and 56 ± 2 kcal/mole, respectively. At higher coverages, the desorption data are complicated by contributions from multiple states. At 100 K, the probability of adsorption of oxygen is approximately 0.2, a value which is maintained to rather high surface coverages due to the precursor nature of the adsorption kinetics.

2. The Adsorption of Hydrogen on the (111) Surface of Rhodium, J. T. Yates, Jr., P. A. Thiel and W. H. Weinberg (in preparation).

The adsorption and desorption kinetics of hydrogen on Rh(111) have been

studied using TDS. The adsorption of hydrogen at temperatures below 175 K occurs with a probability of approximately 0.2. At low surface coverages, a desorption state, exhibiting second-order desorption kinetics, is observed near 375 K. As the coverage of hydrogen increases, the desorption peak shifts to lower temperatures and broadens due to interactional effects in the hydrogen overlayer. No ordering of the hydrogen on the surface is observed by LEED at any coverage. Following adsorption of a mixture of hydrogen and deuterium, isotopic mixing is observed to produce H_2 , D_2 and HD. The desorption of pure deuterium was observed to occur with identical kinetic parameters to pure hydrogen. A kinetic model will be formulated describing both the adsorption and the desorption kinetics. In the case of the latter, the variation with surface coverage of both the pre-exponential factor of the desorption rate coefficient as well as the activation energy of desorption will be evaluated.

3. The Adsorption of Carbon Monoxide on the (111) Surface of Rhodium, E. D. Williams, P. A. Thiel, J. T. Yates, Jr. and W. H. Weinberg (in preparation).

The adsorption of CO on Rh(111) at 90 K has been studied by TDS and LEED. The LEED data suggest that CO adsorbs in a number of ordered structures which are produced at different coverages on the surface. The progression of CO LEED patterns observed, from low to high coverages, is the following: (1) A $(\sqrt{3} \times \sqrt{3})R 30^\circ$ structure at fractional CO coverages (θ_{CO}) below a third of a monolayer, (2) Various "split" (2x2) structures at $\theta_{CO} > 1/3$, and (3) An ordered (2x2) structure at saturation coverage. This progression indicates

a continuous compression of the CO overlayer with increasing CO coverage, a phenomenon which has been observed previously in our laboratory in the case of CO chemisorption on Ir(111) and Ru(001). The relationship between intensity and exposure of both the $(\sqrt{3} \times \sqrt{3})R 30^\circ$ and the (2x2) LEED structures have been measured and will be related to the coverage-exposure functional measured with TDS.

Thermal desorption spectra of CO from Rh(111) yield a first-order desorption feature which shifts to lower temperature and broadens as coverage increases, a result of interadsorbate interactions. The kinetic parameters of the desorption rate coefficient will be evaluated at low coverages, and, if possible, as a function of surface coverage. An upper limit for the ESD cross section of CO on Rh(111) will be evaluated from the measured LEED data. This is of importance to latter work in which the structure of CO in the $(\sqrt{3} \times \sqrt{3})R 30^\circ$ overlayer at $\theta_{CO} = 1/3$ will be determined by LEED.

4. The Coadsorption of Hydrogen and Oxygen on the (111) Surface of Rhodium at 90 K, P. A. Thiel, J. T. Yates, Jr. and W. H. Weinberg (in preparation).

The coadsorption of oxygen and hydrogen on Rh(111) has been studied by TDS, AES and LEED. An important finding in this work is that the coadsorption phenomena which were observed depend strongly upon which of the components of the coadsorbed overlayer is chemisorbed initially, i.e., there is a sensitive dependence upon the order of adsorption.

First, the coverage of hydrogen on Rh(111) has been studied both as a function of oxygen exposure at 90 K prior to hydrogen exposure at 90 K, and as a function of the temperature to which a saturated oxygen overlayer is annealed prior to hydrogen exposure at 90 K. Exposing a clean Rh(111)

surface to oxygen at 90 K prior to exposing it to hydrogen at the same temperature partially blocks hydrogen adsorption and causes the hydrogen to desorb in two new states at approximately 200 K and 400 K. However, annealing the oxygen overlayer allows the adsorption of up to 50% of the saturation amount of hydrogen on clean Rh(111) as judged by TDS. This proves that hydrogen adsorption and desorption are extremely sensitive to the disorder-order-disorder transitions of the oxygen overlayer discussed earlier (Sect. F-1).

Second, the adsorption of oxygen on a Rh(111) surface pre-exposed to hydrogen was investigated. When the Rh(111) surface is saturated with hydrogen at 90 K and then given a saturation exposure of oxygen also at 90 K, the hydrogen desorbs within 10 K of the peak temperature of desorption on the clean surface, with almost no attenuation of the intensity of the desorption peak. This result is surprising in view of the fact that AES indicates that the amount of oxygen adsorbed on the Rh(111) surface saturated with hydrogen is attenuated by only 20% relative to the clean Rh(111) surface. However, *no oxygen thermal desorption occurs* from this coadsorbed overlayer, in marked contrast to the behavior of oxygen on clean Rh(111) as discussed previously in Section F-1. The thermal desorption of oxygen from the surface pre-exposed to hydrogen has been monitored by TDS as a function of hydrogen surface coverage. The pre-adsorbed hydrogen blocks oxygen desorption completely for $\theta_H \geq 0.6$, where θ_H is the fractional coverage of hydrogen relative to saturation coverage. Moreover, LEED measurements indicate that pre-adsorbed hydrogen prevents oxygen from ordering on the surface at temperatures up to the onset of oxygen desorption, 800 K, a temperature at which no hydrogen

remains on the surface. The presence of disordered oxygen on the surface was verified by AES, and TDS was used to show that no detectable water was produced under these experimental conditions. The production of water from hydrogen and oxygen on Rh(111) is discussed below in Section F-6. Consequently, it may be concluded that the presence of hydrogen on Rh(111) influences profoundly the subsequent adsorption of oxygen, even though oxygen desorption occurs at temperatures far higher than those at which hydrogen desorption occurs. The absence of any oxygen thermal desorption from a Rh(111) surface pre-exposed to large amounts of hydrogen may be related to the lack of formation of the ordered (2x2) superstructure which occurs on the clean Rh(111) surface. Additional work relating to this nonreactive coadsorption system will be carried out during the initial stages of support of the renewal grant.

5. The Coadsorption of Carbon Monoxide and Hydrogen on the (111) Surface of Rhodium, P. A. Thiel, J. T. Yates, Jr., E. D. Williams and W. H. Weinberg (in preparation).

Both TDS and LEED have been used to study the nonreactive interaction of hydrogen and CO on Rh(111). When a Rh(111) surface saturated with hydrogen is exposed to CO at 125 K, no displacement of hydrogen is observed. However, the peak in the hydrogen thermal desorption spectrum shifts monotonically to lower temperatures as a function of CO coverage, indicating a decrease in the activation energy for hydrogen desorption. In contrast to this behavior, preadsorption of CO at temperatures below 273 K, followed by a saturation exposure of hydrogen at 125 K, leads to an attenuation of the intensity of the hydrogen thermal desorption spectrum. However, this

attenuation is not accompanied by a shift in the peak temperature indicating that the activation energy for desorption is not changed relative to that which obtains for the clean Rh(111) surface.

As discussed in Section F-3, exposure of the clean Rh(111) surface to CO at 100 K leads to a succession of ordered structures indicative of a continuous compression of the CO overlayer with increasing coverage. The first ordered structure, a $(\sqrt{3} \times \sqrt{3})R 30^\circ$ structure, exhibits a maximum LEED intensity after an exposure of approximately 1.5×10^{-6} torr-sec of CO onto the initially clean surface. Preadsorption of hydrogen causes this intensity maximum to decrease and to shift to *lower* CO exposures. Similarly, post-exposure of hydrogen to a surface on which a well ordered $(\sqrt{3} \times \sqrt{3})R 30^\circ$ CO overlayer exists causes the intensity of the CO superstructure to decrease.

As expected, no methane desorption was observed from the coadsorbed hydrogen and CO overlayers at a sensitivity level of $< 0.5\%$ of desorption of a monolayer of pure CO.

6. The Catalytic Reaction between Adsorbed Oxygen and Hydrogen on the (111) Surface of Rhodium, J. T. Yates, Jr., P. A. Thiel and W. H. Weinberg (in preparation).

Oxygen was found to chemisorb into a disordered state on the (111) surface of Rh near 100 K. As discussed in Section F-1, an activated conversion to an ordered, apparent (2×2) overlayer structure occurs at surface temperatures between approximately 150 and 280 K. Above 280 K, there is a second activated process with an activation energy of 8.2 ± 0.3 kcal/mole which leads to disordered oxygen. The adsorption of oxygen on Rh(111) at 335 K occurs via Langmuir kinetics with a probability of adsorption of approximately 0.6.

During adsorption at this temperature, a mixture of ordered and disordered oxygen is produced with massive conversion to the ordered layer in the final stages of adsorption at exposures of oxygen greater than 5×10^{-6} torr-sec. At fractional surface coverages below half of saturation, the intensity of the $(1, \frac{1}{2})$ LEED beam increases as the square of the fractional surface coverage as expected for the formation of ordered oxygen islands.

The reaction of the ordered oxygen overlayer with hydrogen to produce water occurs rapidly above 275 K with hydrogen pressures in the 10^{-8} to 10^{-6} torr region. The reaction exhibits first order kinetics in hydrogen pressure, implying a trapping mechanism for adsorbed hydrogen on the ordered oxygen overlayer, i.e., irreversible adsorption of hydrogen. The activation energy for the removal of ordered oxygen by reaction with hydrogen is 5.3 kcal/mole, and the reaction cross section is approximately 250 \AA^2 (the pre-exponential factor of the reaction rate coefficient). This large cross section for the loss of ordered oxygen indicates that near saturation coverage of oxygen, massive disordering occurs for small decreases in oxygen coverage during reaction. This observation is consistent with the earlier observation of massive oxygen ordering during the final stages of oxygen adsorption at 335 K. A Langmuir-Hinshelwood mechanism for the reaction is suggested by the observation of H_2O , HDO and D_2O reaction products when mixtures of gaseous hydrogen and deuterium were used to react with the chemisorbed oxygen.

G. References (Papers Resulting from the Support of Grant DAHC04-75-G-0170)

1. "A Determination of Surface Relaxation from Low-Energy Electron Diffraction Using a Fourier Transformation Method," S. L. Cunningham, C.-M. Chan and W. H. Weinberg, Phys. Rev. B (15 July 1978).
2. "Structural Determinations from LEED Spectra by Data Reduction," G. L. Griffin, S. L. Cunningham and W. H. Weinberg, Bull. Am. Phys. Soc. 21, 320 (1976).
3. "Determining Surface Relaxation from LEED Via a Transform Method," S. L. Cunningham, C.-M. Chan and W. H. Weinberg, J. Vac. Sci. Technol. 14, 312 (1977).
4. "Determination of Surface Relaxation of fcc Metals by LEED," C.-M. Chan, S. L. Cunningham, M. A. Van Hove and S. P. Withrow, Bull. Am. Phys. Soc. 22, 357 (1977).
5. "An Analysis of the Structure of the Iridium (111) Surface by Low-Energy Electron Diffraction," C.-M. Chan, S. L. Cunningham, M. A. Van Hove, W. H. Weinberg and S. P. Withrow, Surface Sci. 66, 394 (1977).
6. "Surface Relaxation of Ni(110), Al(110) and Ag(110) Determined by the Convolution Transform Method," C.-M. Chan, S. L. Cunningham, M. A. Van Hove and W. H. Weinberg, Surface Sci. 67, 1 (1977).
7. "The Geometrical and Vibrational Properties of the Rh(111) Surface," C.-M. Chan, P. A. Thiel, J. T. Yates, Jr. and W. H. Weinberg, Surface Sci. (in press, 1978).
8. "The State of the Surface of Martensitically Transforming Cobalt Single Crystals," R. Alsensz, B. W. Lee, A. Ignatiev and M. A. Van Hove, Solid State Commun. 25, 641 (1978); Bull. Am. Phys. Soc. 22, 357 (1977).
9. "Determination of the Atomic Arrangement of the Unreconstructed Ir(110) Surface by Low-Energy Electron Diffraction," C.-M. Chan, S. L. Cunningham, K. L. Luke, W. H. Weinberg and S. P. Withrow, Surface Sci. (accepted, 1978).
10. "Analysis of Atomic Locations by LEED for a Submonolayer of Dissociated Hydrogen on a Ni(111) Surface," M. A. Van Hove, G. Ertl, W. H. Weinberg, K. Christmann and H. J. Behm, Bull. Am. Phys. Soc. 22, 356 (1977).
11. "Analysis of Atomic Locations by LEED for a Submonolayer of Dissociated Hydrogen on a Ni(111) Surface," M. A. Van Hove, G. Ertl, W. H. Weinberg, K. Christmann and H. J. Behm, Proc. 7th Internal. Vac. Congress and 3rd Internal. Conf. Solid Surfaces, p. 2415, 1977.
12. "Geometry of Hydrogen Chemisorption on Ni(111) Determined by Low-Energy Electron Diffraction," M. A. Van Hove, G. Ertl, K. Christmann, H. J. Behm and W. H. Weinberg, Phys. Rev. Letters (submitted, 1978).

13. "The Structure of the c(2x2) Oxygen Overlay on the Unreconstructed (110) Surface of Iridium," C.-M. Chan, K. L. Luke, M. A. Van Hove, W. H. Weinberg and S. P. Withrow, *Surface Sci.* (accepted, 1978).
14. "Determining the Angles of Incidence in a LEED Experiment," S. L. Cunningham and W. H. Weinberg, *Rev. Sci. Instrum.* 49, 752 (1978).
15. "Determination of Adatom Interaction Energies by a Monte Carlo Calculation: Oxygen on W(110)," E. D. Williams, S. L. Cunningham and W. H. Weinberg, *J. Vac. Sci. Technol.* 15, 417 (1978).
16. "Determination of Adatom-Adatom Interaction Energies: Application to Oxygen Chemisorbed on the Tungsten (110) Surface," E. D. Williams, S. L. Cunningham and W. H. Weinberg, *J. Chem. Phys.* 68, 4688 (1978).
17. "An Analysis of Thermal Desorption Mass Spectra," C.-M. Chan, R. Aris and W. H. Weinberg, *Appl. Surface Sci.* 1, 360 (1978).
18. "An Analysis of Thermal Desorption Mass Spectra, II," C.-M. Chan and W. H. Weinberg, *Appl. Surface Sci.* 1, 377 (1978).
19. "Electron Beam Induced Desorption and Dissociation of CO Chemisorbed on Ir(110)," M.-L. Shek, S. P. Withrow and W. H. Weinberg, *Surface Sci.* 72, 678 (1978).
20. "Concentration Dependence of Inelastic Electron Tunneling Spectroscopy," S. L. Cunningham, W. H. Weinberg and J. R. Hardy, *Bull. Am. Phys. Soc.* 22, 256 (1977).
21. "Effect of Cooperative Behavior on Molecular Vibrational IETS Peak Intensities," S. L. Cunningham, W. H. Weinberg and J. R. Hardy, in *Inelastic Electron Tunneling Spectroscopy*, Ed., T. Wolfram, Springer-Verlag, Berlin, p. 125, 1978.
22. "Dependence of the Inelastic Electron Tunneling Intensity on Adsorbate Concentration," S. L. Cunningham, W. H. Weinberg and J. R. Hardy, *Appl. Surface Sci.* (submitted, 1978).
23. "Surface Reconstruction of a Two-Band Crystal: I. Green's Function Formalism," W. Ho, S. L. Cunningham, W. H. Weinberg and L. Dobrzynski, *Appl. Surface Sci.* 1, 33 (1977).
24. "Surface Reconstruction of a Two-Band Crystal: II. Model Results," W. Ho, S. L. Cunningham, W. H. Weinberg and L. Dobrzynski, *Appl. Surface Sci.* 1, 44 (1977).
25. "Chemisorption-Induced Interaction between Electronic Levels of a Two-Level Adsorbate on an fcc(100) Surface," M.-L. Shek, S. L. Cunningham and W. H. Weinberg, *Surface Sci.* (submitted, 1978).
26. "A Method of Continuously Measuring Work Function Changes," J. L. Taylor and W. H. Weinberg, *J. Vac. Sci. Technol.* (accepted, 1978).
27. "Chemisorption of Carbon Monoxide on the (110) Surface of Iridium," J. L. Taylor and W. H. Weinberg, *J. Vac. Sci. Technol.* 15, 590 (1978).